

## Morphology and dc-electric properties of p-terphenyl thin films

This article has been downloaded from IOPscience. Please scroll down to see the full text article.

2008 J. Phys. D: Appl. Phys. 41 155411

(<http://iopscience.iop.org/0022-3727/41/15/155411>)

View [the table of contents for this issue](#), or go to the [journal homepage](#) for more

Download details:

IP Address: 128.3.131.180

The article was downloaded on 11/11/2010 at 23:46

Please note that [terms and conditions apply](#).

# Morphology and dc-electric properties of p-terphenyl thin films

S W Tkaczyk

Institute of Physics, J Dlugosz University, Al. Armii Krajowej 13/15, 42-200 Częstochowa, Poland

Received 4 February 2008, in final form 28 May 2008

Published 11 July 2008

Online at [stacks.iop.org/JPhysD/41/155411](http://stacks.iop.org/JPhysD/41/155411)

## Abstract

Dc conductivity investigations were performed for polycrystalline p-terphenyl thin films, including temperature dependences. The conductivity measurements were done for samples with thickness 1.7–12.5  $\mu\text{m}$  at polarizing voltages varying in the range 0–200 V in the temperature range 15–325 K. The investigated thin films were supplied with gold and aluminium electrodes. The obtained results and their analysis indicate that the injection of charge from the electrodes into the area of the investigated films proceeds by field- and thermo-emission dependent on the temperature and electric field values. The charge transport through the material's bulk is controlled by trapping levels situated within the energy gap area and is described by the hopping mechanism and the Poole–Frenkel phenomenon. The determined values of the activation energies are of the order of the thermal energy ( $kT$ ), which is equivalent to the non-activating hopping energy, close to 0.06 eV in the temperature range 15–200 K. In this temperature range dc conductivity of doping semiconducting character is observed. It is crucial that within the temperature range 200–325 K the conductivity is metallic-like and the activation energy value is about 0.6 eV.

## 1. Introduction

Traditionally polycrystalline films possess many structural defects, which form many trapping levels within the forbidden band. As a consequence all the properties related to the occupation of these levels in the external fields will be crucially dependent on the number of defects and energy positions of the virtual density of states. These levels are particularly crucial for organic and molecular crystalline materials [1]. Moreover, they can even change the local symmetry forming a non-centrosymmetry [2] leading to nonlinear optical effects.

In the low-ordered and low-dimensional structures, instead of a well-defined energy gap, we deal with an area characterized by a high density of trapping within energy gap levels. As a consequence the energy position of the Fermi energy is also shifted. Due to the presence of microcrystallites there occur many nano-confined states, which usually lead to flattening in the  $k$  space of the band energy dispersions [3]. One can say that the electronic structure of the polycrystalline films is intermediate between amorphous-like materials and low-dimensional crystallites. At the same time polycrystalline materials themselves are convenient modelling objects for hopping conductivity approaches for a wide range of temperatures and electric fields. Deviations from the

classical transport of thermally activated electrons that were observed in the low-ordered materials became principal for the hopping model with a variable range proposed by Mott in 1968 [4, 5, 9, 10]. The charge transport mechanism bulk materials cannot be described sufficiently by the equation  $\ln \sigma = f(T^{-1/4})$ .

Even assuming that the distribution of trapping levels in the sample's bulk is homogeneous and their activation energy changes linearly does not simplify the problem.

The physical properties of the investigated materials are crucial for the observed conductivity mechanism. Two- or three-dimensional hopping is observed depending on:

- (1) how the density of trapping states is changed with temperature,
- (2) what is the dimensionality of the investigated sample, especially its thickness,
- (3) inhomogeneities in the sample's bulk,
- (4) the existence of multi-photon processes, and
- (5) the existence of Coulomb interaction during charge carrier transport (the influence of bulk on the value of current conducted in the material).

In high electric fields or in the case when the system electron material is not a perfect injecting contact the current flowing

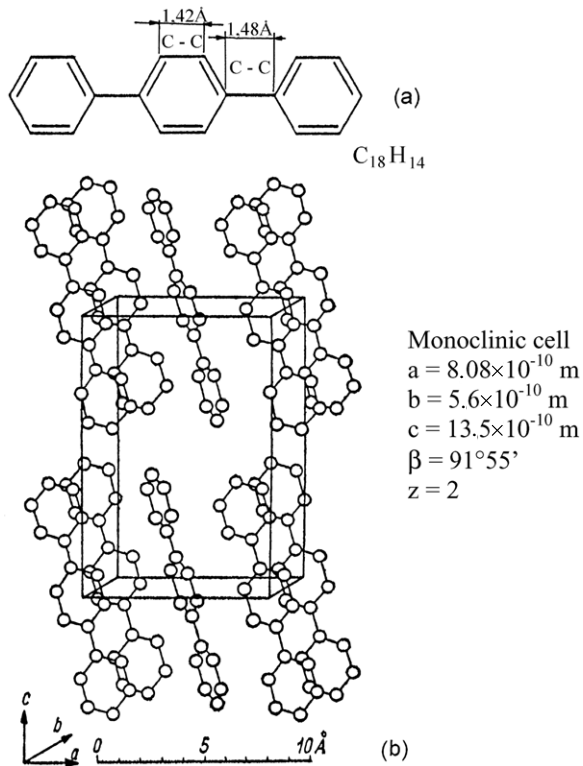


**Figure 1.** Chemical formula of p-terphenyl (p-diphenylbenzene): (a) single molecule and (b) crystal unit cell.

through the sample is controlled by contact as well as bulk phenomena appearing in the material.

This paper is devoted to the study of p-terphenyl belonging to the p-phenyl homologue row.

In section 2 we present morphological parameters of films of different thicknesses. Section 3 analyses the influence of the morphology presented in section 2 together with film sizes on the transport properties.

## 2. Experiment

The material under investigation was clean p-terphenyl, produced by FLUKA, of  $C_{18}H_{14}$  stoichiometry and with molecular mass equal to 230.3101. The p-terphenyl molecule is flat and consists of three benzene rings lying in a straight line (figure 1(a)). The C–C bond lengths in the benzene ring and between the rings are about  $1.42 \times 10^{-10} \text{ m}$  and  $1.48 \times 10^{-10} \text{ m}$ , respectively. The p-terphenyl crystal unit cell is monoclinic with the following crystallographic parameters:  $a = 8.08 \times 10^{-10} \text{ m}$ ,  $b = 5.6 \times 10^{-10} \text{ m}$ ,  $c = 13.5 \times 10^{-10} \text{ m}$ ,  $\beta = 91^\circ 55'$  (figure 1(b)) [6–8].

The p-terphenyl samples used in the dc conductivity measurements were obtained as polycrystalline thin films. The samples were obtained through the vacuum sublimation process on either BK-7 glass or gold substrates supplied with gold electrodes. The sublimation process was controlled with regard to

- (1) the rate of the layers growth,
- (2) the deposition process temperature,

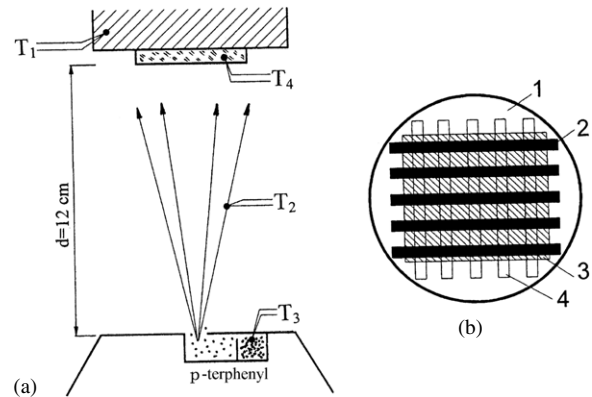


**Figure 2.** (a) Schematic arrangement for the production of p-terphenyl thin films.  $T_1$ ,  $T_2$ ,  $T_3$ ,  $T_4$ —copper–constantan thermocouples measuring temperatures of substrate, sublimation chamber, evaporator and sample, respectively. (b) sample arrangement: 1—substrate (BK-7 glass), 2—upper electrode (aluminium), 3—p-terphenyl film and 4—bottom electrode (gold).

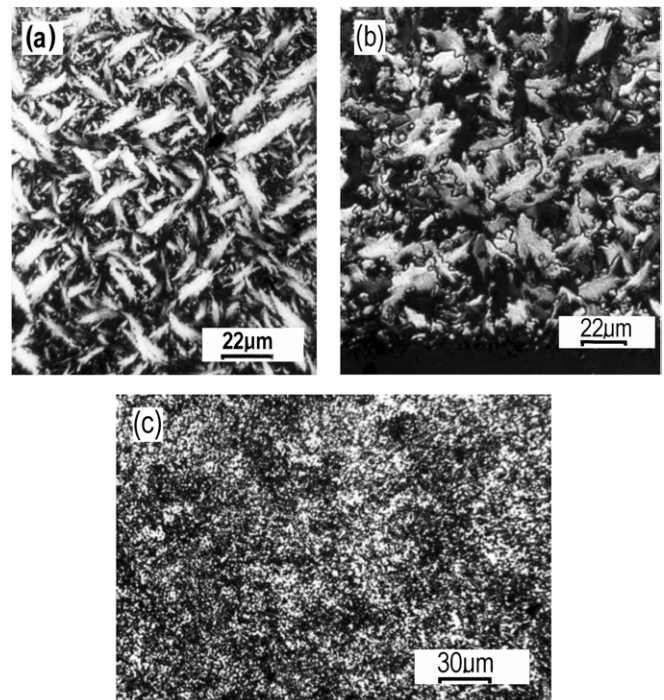


**Figure 3.** Polarizing microscope pictures taken for transmitting light with a crossed polarizer and an analyzer ( $d$ —thickness of layer p-terphenyl,  $p$ —magnification). (a) p-terphenyl on the BK-7 glass substrate;  $d = 2.45 \mu\text{m}$ ;  $p = 440$ ;  $T_1 = 301.4 \text{ K}$ ;  $T_2 = 306.7 \text{ K}$ ;  $T_3 = 403 \text{ K}$ ;  $T_4 = 303 \text{ K}$ . (b) p-terphenyl on the BK-7 glass substrate;  $d = 12.5 \mu\text{m}$ ;  $p = 460$ ;  $T_1 = 301.4 \text{ K}$ ;  $T_2 = 307 \text{ K}$ ;  $T_3 = 402.3 \text{ K}$ ;  $T_4 = 303 \text{ K}$  (visible layers, edges and glass BK7). (c) p-terphenyl on the gold substrate;  $d = 12.5 \mu\text{m}$ ;  $p = 328$ ;  $T_1 = 301.1 \text{ K}$ ;  $T_2 = 308 \text{ K}$ ;  $T_3 = 383 \text{ K}$ ;  $T_4 = 304 \text{ K}$ .

- (3) the pressure inside the chamber and
- (4) the deposition rate was about  $30 \text{ nm s}^{-1}$ .

Figure 2(a) presents the thin film sublimation process together with the temperature check points. In figure 2(b) the system of electrodes and the method of giving a proper shape to the investigated material deposited on the glass substrate (BK-7) are presented. The crystalline grains sizes occurred in the

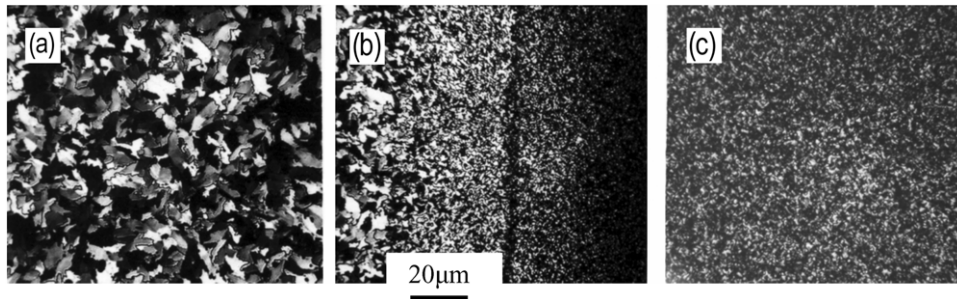


**Figure 4.** Pictures of p-terphenyl thinfilms deposited on a glass or gold substrate. (a) p-terphenyl on glass substrate (Pt/BK-7). (b) Left side: p-terphenyl on PT/BK-7 glass substrate, right side: p-terphenyl on PT/Au substrate. (c) p-terphenyl on gold substrate (PT/Au).

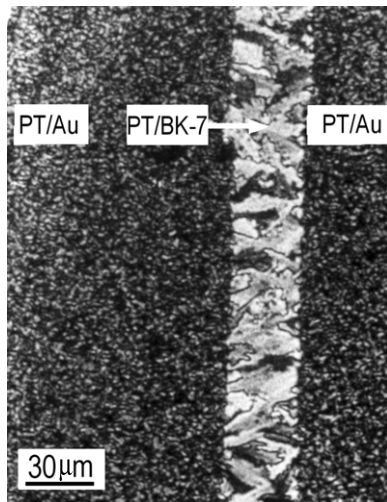


**Figure 5.** Pictures of the p-terphenyl thin films deposited on a glass or gold substrate taken with the use of a polarizer microscope in transmitted light with a crossed analyzer and a polarizer. Left and right sides: PT/Au—small crystallites. Central part of the picture: PT/BK-7—large crystallites.  $T_1 = 301.4$  K;  $T_2 = 306.7$  K;  $T_3 = 402.3$  K;  $T_4 = 302.6$  K.

obtained thin films depending on sublimation conditions, such as the process temperature (in various part of the sublimation chamber), the rate of p-terphenyl deposition and the type of substrate [6–8].

In figures 3 and 4 pictures of p-terphenyl thin films deposited on glass and gold substrates are presented. It is obvious that the size of the crystalline grains of a thin film deposited on the glass substrate depends on the p-terphenyl film thickness.

From figures 3(c), 4(c) and 5 one can see that the size of the crystalline areas is rather small and these samples might be considered as nanocrystals. Figure 5 shows the evidence that the substrate type has a significant influence on the p-terphenyl polycrystalline grain size. The width of the glass substrate in this case was about  $35 \mu\text{m}$ .

The thickness of the investigated p-terphenyl polycrystalline films was varied in the range  $1.5\text{--}15 \mu\text{m}$ . Measurements consisted of the evaluation of current flowing through the sample bulk between the gold and the aluminium electrodes. The measurements were carried out for different electrode polarities in the voltage range  $0\text{--}200$  V in the temperature range  $15\text{--}325$  K. Such a wide range of temperatures was, for the first

time to our knowledge, used for investigations of p-terphenyl thin films. The equipment used in the dc conductivity experiment was similar to that described in [6].

### 3. Results and discussion

The obtained results of the study of polycrystalline p-terphenyl thin films dc conductivity allow us to conclude that the charge transport through the material's bulk is caused by different conductivity mechanisms. The character of the conductivity depends on the electric field value, temperature and electrode polarities. The  $I\text{--}V$  characteristics shown in figure 6 show us the non-ohmic character of conductivity in the investigated material. Figures 6(a) and (b) show that switching of the electrode's polarity does not change the shape of the  $I\text{--}V$  characteristics, i.e. does not influence the conductivity character. We can conclude that for the sample of  $1.73 \mu\text{m}$  thickness in a wide range of temperatures the sample behaves like a varistor and the conductivity is a bulk process (figures 6(a) and (b)). Another sample,  $6 \mu\text{m}$  thick, in a wide range of temperatures ( $16\text{--}260$  K) possesses conductivity character independent of the electrode polarity (see figure 6(c)).

In the case of p-terphenyl  $8.5 \mu\text{m}$  thick the conductivity character is analogous to the semiconducting diode (figure 6(d)). This may be due to the formation of a quasi-Schottky barrier. When polarity is Au(–) we observe the current flowing in the conductivity direction while with polarity Au(+) the direction is opposite. Such an effect is observed in a wide range of temperatures ( $16\text{--}325$  K). The character of conductivity is dependent on the mechanisms of charge transport through the investigated materials. For films of thickness about  $2 \mu\text{m}$  the dominant process is the current limited by the screening effects of trapping levels. Simultaneously there occurs an effect described by the Poole–Frenkel law. Another influence may be related to the carrier transport from the electrodes.

Using the  $\ln I = f(1/kT)$  relation ( $k$  the Boltzmann constant,  $T$  the temperature,  $I$  the current) we determined the dc conductivity energy for various sample polarizing voltages for samples of different thicknesses. Typical  $\ln I = f(1/kT)$  features are shown in figure 7 [6–8].

For each of the  $\ln I = f(1/kT)$  p-terphenyl characteristics it is possible to separate three areas with different slopes.

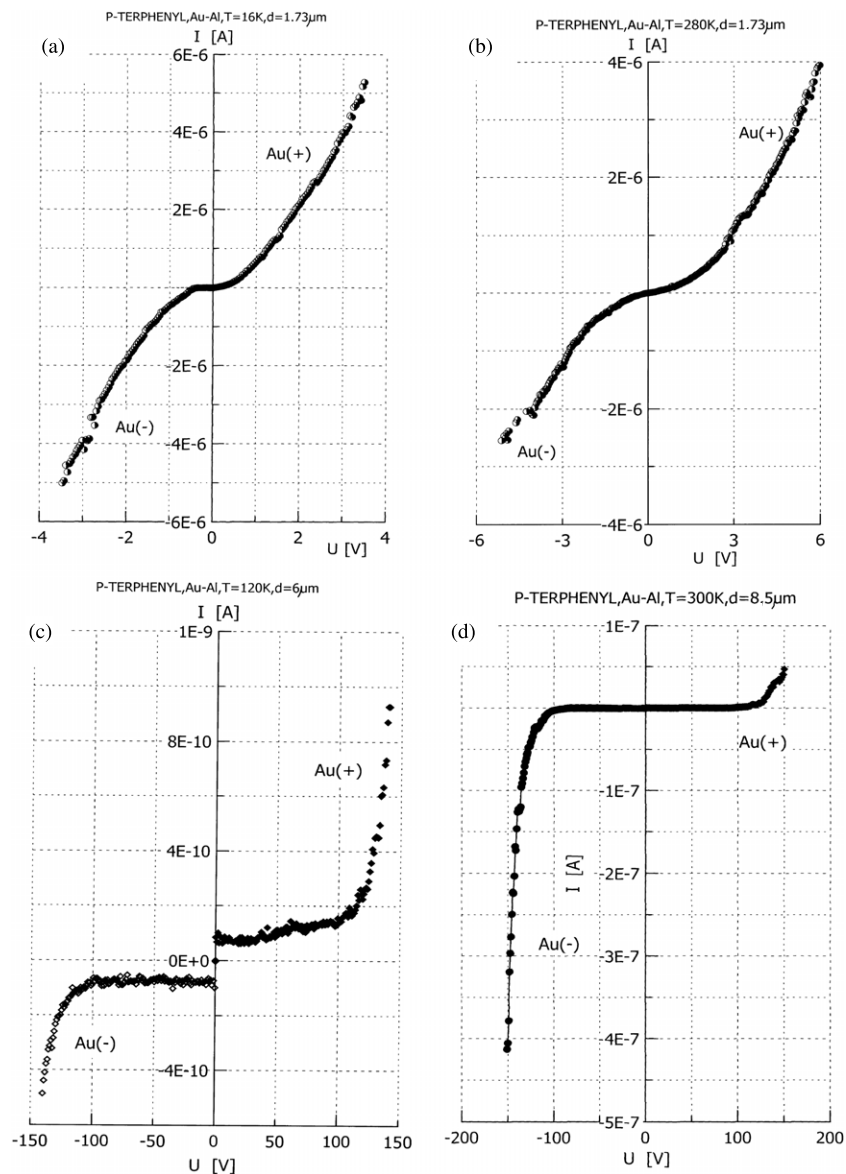


**Figure 6.** Current–voltage dependences for polycrystalline films of p-terphenyl supplied with Au–Al electrodes with various electrode polarities. PT film thickness and sample temperature, respectively: (a)  $1.73\ \mu\text{m}$ , 16 K, (b)  $1.73\ \mu\text{m}$ , 280 K, (c)  $6\ \mu\text{m}$ , 120 K and (d)  $8.5\ \mu\text{m}$ , 300 K.

The slope magnitude is the measure of the activation energy for conductivity.

For example, the  $E_3$  area in figure 7(a) or  $E_2$  in figure 7(b) correspond to the energy of hopping conductivity through localized trapping states formed by structural defects. The value of the activation energy for these mechanisms is equal to about  $kT$  and is not shown in figures 8–12. The  $E_2$  area seen in figure 7(b) is characterized by activation energies 0.01–0.06 eV in the temperature range 100–220 K. In this area the investigated material behaves like a semiconductor. The activation energy values are greater than 0.1 eV but less than 0.7 eV.

Figures 8–12 present the dependence of activation energies  $E_a$  versus the applied voltage. The low values of activation energy (below 0.1 eV) are independent of voltage, which corresponds to the conductivity with the participation

of the hopping mechanism with the participation of donor bands. An increase in activation energy (figures 9–12) for region  $E_1$  indicates that with the increase in the voltage the trapping levels are depopulated with higher activation energies. With a further increase in the voltage ionization of the trapping levels takes place in accordance with the Poole–Frenkel law, i.e. the activation energies effectively decrease with the applied voltage. This is clearly seen in figures 10–12.

Such parameters correspond to metal-like conductivity. In figure 13 the dependence of the resistivity ( $R$ ) of the p-terphenyl thin film with respect to room temperature ( $R_1$ ) is shown,  $T = 295\ \text{K}$ . It is seen from the figure that the investigated material had semiconductor-like features below 80 K, while in the temperature range over 80 K it showed metal-like features.

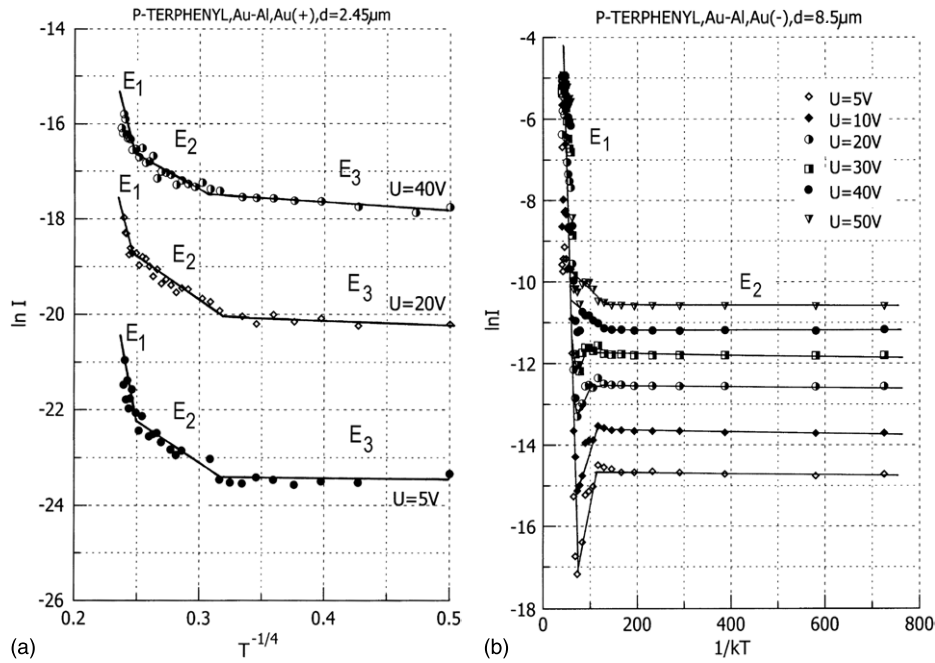


Figure 7. The dependence  $\ln I = f(1/kT)$  for p-terphenyl films: (a) sample thickness  $2.45 \mu\text{m}$ , Au–Al; Au(–) and (b) sample thickness  $8.5 \mu\text{m}$ , Au–Al; Au(–).

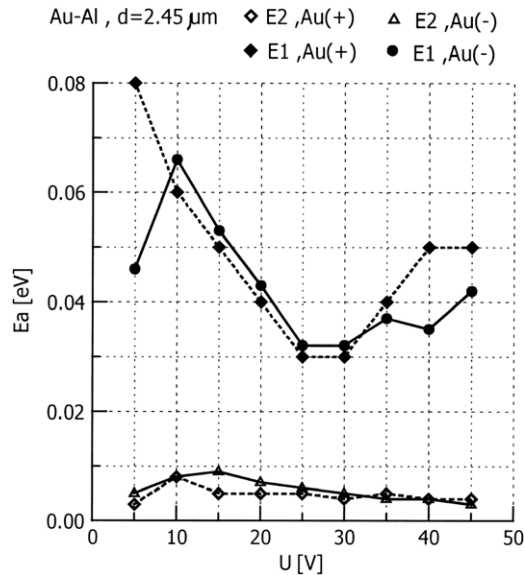


Figure 8. Activation energy values for polycrystalline p-terphenyl  $2.45 \mu\text{m}$  thick (Au–Al electrodes) at different voltages polarizing the sample.  $T \in 110 \text{ K}–320 \text{ K}$ .

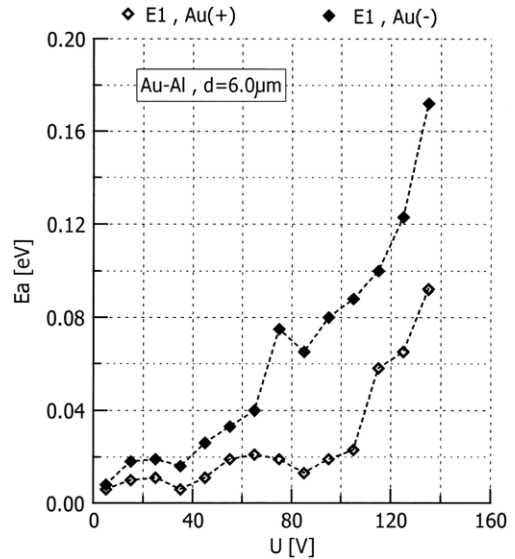
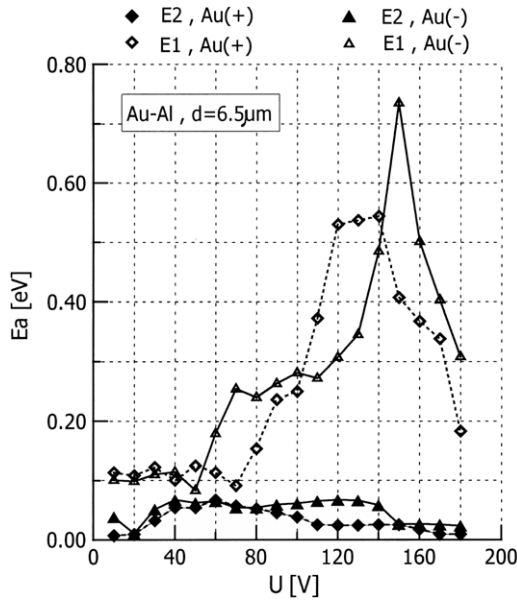


Figure 9. Activation energy values at different voltages polarizing the sample  $T \in 110 \text{ K}–320 \text{ K}$ .

At low temperatures the transport of charge carriers, whose concentration from the  $I = f(U^2/d^3)$  dependence was found to be equal to  $n = 0.4–0.5 \times 10^{22} \text{ m}^{-3}$ , takes place through the hopping between localized states (prevalingly situated on the boundaries of crystalline grains) over the potential barriers separating the areas. An external electric field generated by the electrode voltage lowers the barrier height, according to the Poole–Frenkel law. In this case, the hopping model is supported by rectilinear characteristics  $\ln \sigma = f(T^{-1/3})$  and  $\ln \sigma = f(T^{-1/4})$ . It is evident

(figure 14) that we can consider two- and three-dimensional hopping [2, 8–11]. The hopping mechanism is dominant at temperatures below 120 K (figures 14(a) and (b)) [12].

While the external electric field increases the height of the potential barrier near trapping levels is decreased (Poole–Frenkel effect). The Poole–Frenkel phenomenon is seen in the typical shape of the  $\ln I = f(U^{1/2})$  curve and the lowering activation energy while the supplied voltage increases (figure 15). The presence of the phenomenon is also confirmed by the shape of the  $\log(I d^2 / U^2) = f(1/T)$  characteristics—figure 16. The rectilinear section of the curves suggests



**Figure 10.** Activation energy values at different voltages polarizing the sample.  $E_1 - T \in (180 \text{ K} - 320 \text{ K})$ ,  $E_2 - T \in (100 \text{ K} - 180 \text{ K})$ .

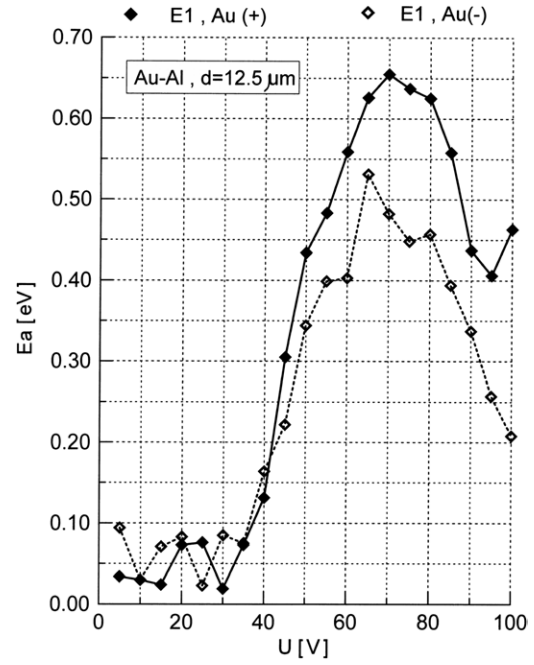


**Figure 12.** Activation energy values at different voltages polarizing the sample.  $E_1 - T \in (180 \text{ K} - 320 \text{ K})$ .

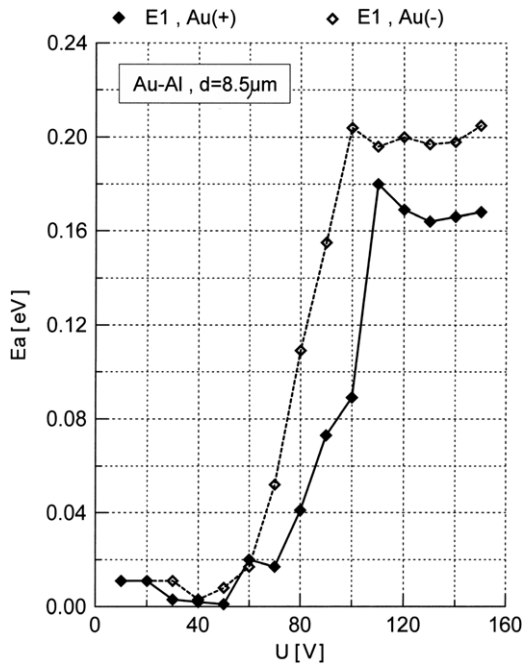


**Figure 11.** Activation energy values at different voltages polarizing the sample.  $E_1 - T \in (180 \text{ K} - 320 \text{ K})$ .

that electric charge tunnels between defect originated trapping states [5–8].

It is necessary to add that the Poole–Frenkel effect is a bulk effect, i.e. effective conductivity is a function of the thickness and the voltage:

$$\sigma = \sigma_0 \exp(\beta_{P-F} E^{1/2} / k_B T),$$

where  $\beta_{P-F} = (\epsilon^3 / \pi \epsilon \epsilon_0)^{1/2}$  Poole–Frenkel coefficients. The poor linearity in figure 15 in the dependences  $\ln I = f(U^{1/2})$

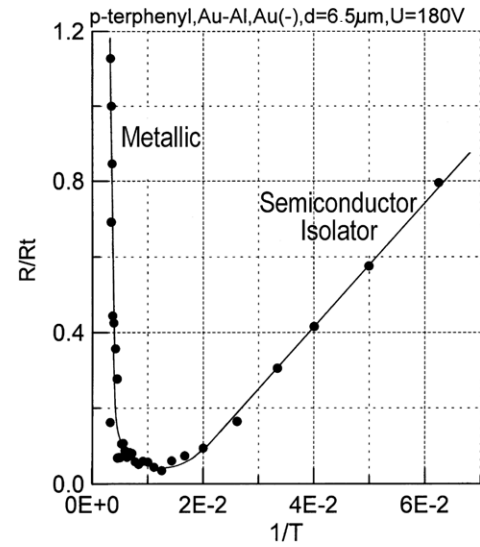


**Figure 13.** The dependence  $R/R_t = f(T^{-1})$  for polycrystalline p-terphenyl layers; the sample thickness:  $6.5 \mu\text{m}$ ,  $U = 180 \text{ V}$ ; Au–Al; Au(–);  $R_t$ —layer resistivity at 295 K.

indicate the occurrence of the Poole–Frenkel effect [13, 14] and on the changes in the activation energies versus the applied voltage.

The injection of charge carriers from the electrodes to the investigated material bulk proceeds through thermo- and field emission. Figure 17 shows that a high voltage determines the injection of charge from an electrode to the p-terphenyl bulk in the field emission (tunnelling) process and this phenomenon is dominant. This is a contact-originated phenomenon confirmed additionally in figure 18. It is seen that for the case of high electric field ( $U > 60 \text{ V}$ ) the Schottky phenomenon

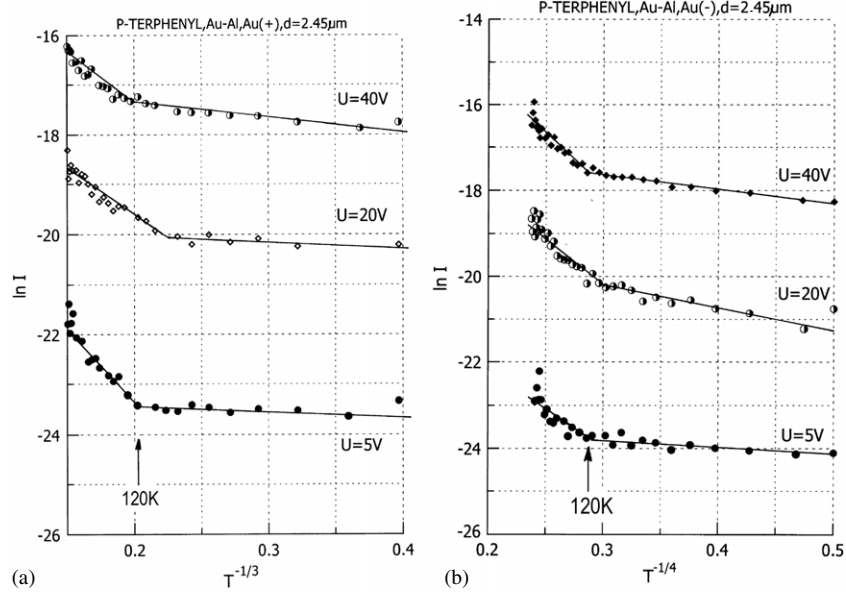


**Figure 14.** The  $\ln I = f(T^{-1/3})$  (a) and  $\ln I = f(T^{-1/4})$  (b) curves obtained for polycrystalline p-terphenyl layers 2.45  $\mu\text{m}$  thick; Au–Al electrodes.

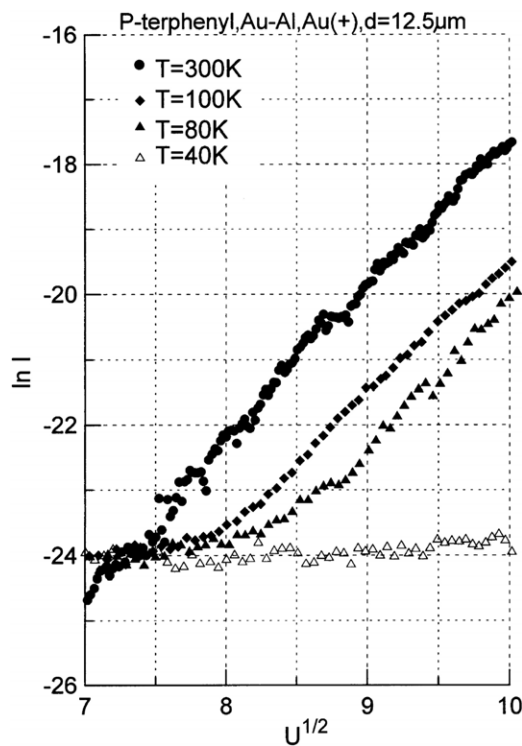


**Figure 15.** The  $\ln I = f(U^{1/2})$  dependence for p-terphenyl layers 12.5  $\mu\text{m}$  thick at different temperatures; Au–Al electrodes, Au(+).

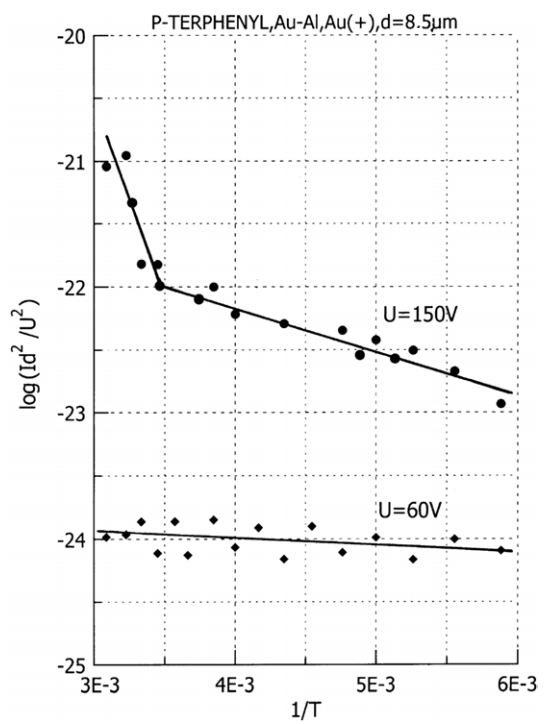


**Figure 16.** The  $\log(I d^2 / U^2) = f(1/T)$  dependence for p-terphenyl 8.5  $\mu\text{m}$  thick; Au–Al electrodes, Au(+).

is dominant. In the case of lower electric fields thermo-emission of charge from the electrodes to the sample’s bulk is also important (figure 17). The dependence shown in figure 17 (Fowler–Nordheim curve) illustrates the contribution of the investigated material’s surface and contact with metal electrodes in the charge transport into the bulk [5–8]. Additionally electric field induced dipole moments may give some contributions [15].

#### 4. Conclusions

During the investigations of the polycrystalline p-terphenyl films it was established that there exists more than one mechanism of conductivity in a wide range of temperatures and electric fields. In low electric fields when the temperature is less than 200 K charge transport occurs through non-activated hopping (two- and three-dimensional), which is confirmed by the small value of activation energy.

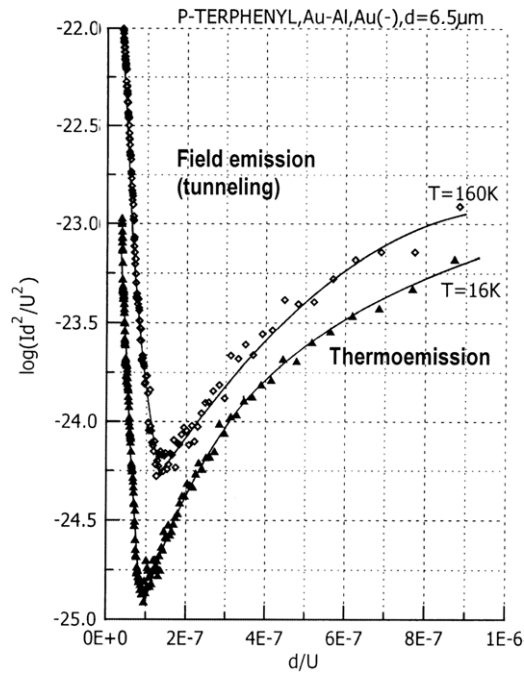


Figure 17. Fowler-Nordheim plot  $\ln(I d^2 / U^2) = f(d / U)$  for p-terphenyl layers 6.5  $\mu\text{m}$  thick; Au-Al, Au(+).

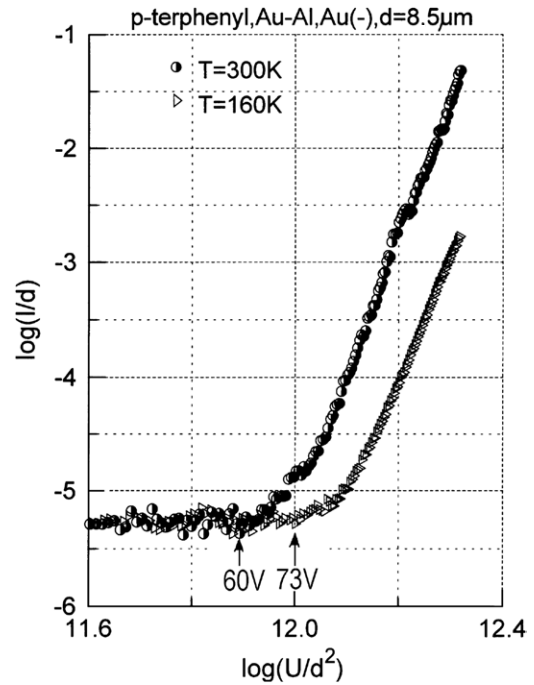


Figure 18. The  $\log(I/d) = f[\log(U/d^2)]$  curve characteristic of the Schottky phenomenon (rectilinear segments of the curves corresponding to a higher voltage) taken at different temperatures.

References

[1] Tkaczyk S W, Kityk I V and Schiffer R 2002 *J. Phys. D: Appl. Phys.* **35** 563-9

[2] Kityk I V, Marciniak B and Mefleh A 2001 *J. Phys. D: Appl. Phys.* **34** 1-4

[3] Kityk I V 2003 *Semicond. Sci. Technol.* **18** 1001-9

[4] Mott N F 1971 *Phil. Mag.* **24** 911

[5] Voegelé V, Kalbitzer S and Boringer K 1985 *Phil. Mag. B* **52** 153

[6] Selvakumar S, Sivaji K, Balamurugan N, Arulchakkaravarthi A, Sankar S, Venkateswaran C and Ramasamy P 2005 *J. Cryst. Growth* **275** e265

[7] Świątek J and Tkaczyk S 1993 *Mol. Cryst. Liq. Cryst.* **228** 195

[8] Kityk I V 2001 *J. Non-Cryst. Solids* **292** 184-201

[9] Tkaczyk S W 1996 *Electron Technol.* **29** 232

[10] Tkaczyk S W 2000 *Synth. Met.* **109** 249

[11] Tkaczyk S W and Świątek J 2000 *Synth. Met.* **106** 255

[12] Tkaczyk S and Kityk I V 2005 *Appl. Surf. Sci.* **241** 287

[13] Simmons I G 1968 *Phys. Rev.* **166** 912

[14] Sze S M 1981 *Physics of Semiconductor Devices* (New York: Wiley)

[15] Kityk I V, Makowska-Janusik M, Gondek E, Krzeminska L, Danel A, Plucinski K J, Benet S and Sahraoui B 2004 *J. Phys.: Condens. Matter.* **16** 231-9